DOI:10.22337/2587-9618-2023-19-3-92-113

SEISMIC FRAGILITY EVALUATION OF SOIL-PILE-STRUCTURE INTERACTION EFFECTS SUBJECTED TO MAINSHOCK-AFTERSHOCK RECORDS

Souheyla Saddouki, Djarir Yahiaoui, Rafik Demagh

LGC-ROI, Department of Civil Engineering, Faculty of Technology, University of Batna 2, Batna, ALGERIA

Abstract: In most current seismic design on bridges, only mainshock actions are considered without incorporating the effect of mainshock-aftershock (MA) sequences and interaction soil-pile. However, a large mainshock usually triggers numerous aftershocks in a short period. This paperstudy the effect of mainshock-aftershock sequences on the behavior of interaction Soil-pile-structure system (**ISPS**). abeam on nonlinear Winkler foundation (BNWF) model is usingand subjected to non-linear static analysis and incremental dynamic analysis (IDA) leading finally to the fragility curves which are developed. These analyses aim to capture the collapse state of structures under aftershock events preceded by various mainshock levels. Results obtained from capacity curve, incremental dynamic and fragility curves of ISSP system. The analytical results show that in the MA sequences, for dense soil the vulnerable of mainshock-aftershock (MS-AS) loading are more damage due to mainshock loading for all diameter of the pile and the mass. For soft soil are more vulnerable to damage due to mainshock-aftershock (MS-AS) loading. But in the stiff clay the effect of mainshock-aftershock (MS-AS) loading for all the diameter of pile and for masse are neglected.

Keywords: bridge, interaction soil-pile-structure, Winkler foundation, dynamic analysis, fragility curves, mainshock-aftershock

ОЦЕНКА СЕЙСМИЧЕСКОЙ НЕУСТОЙЧИВОСТИ ЭФФЕКТОВ ВЗАИМОДЕЙСТВИЯ ГРУНТ-СВАЯ-КОНСТРУКЦИЯ, ПОДВЕРЖЕННЫХ ЗАПИСЯМ ОСНОВНЫХ ТОЛЧКОВ И АФТЕРШОКОВ

Сухейла Саддуки, Джарир Яхиауи, Рафик Демаг

LGC-ROI, Департамент гражданского строительства, Технологический факультет Университета Батны 2, г. Батна, АЛЖИР

Аннотация: В большинстве современных сейсмических расчетов мостов учитываются только основные толчки без учета воздействия последовательностей основных толчков и афтершоков (МА) и взаимодействия грунта и сваи. Однако сильный главный толчок обычно вызывает многочисленные повторные толчки за короткий период. В данной статье исследуется влияние последовательностей основных толчков и афтершоков на поведение системы взаимодействия «грунт-свая-сооружение» (ИСПС). балка на нелинейном фундаменте Винклера (BNWF) используется и подвергается нелинейному статическому анализу и инкрементному динамическому анализу (IDA), что в конечном итоге приводит к построению кривых хрупкости. Эти анализы направлены на то, чтобы зафиксировать состояние обрушения конструкций при афтершоковых событиях, которым предшествовали основные толчки различных уровней. Результаты, полученные из кривой емкости, кривых инкрементной динамики и кривых хрупкости системы ISSP. Аналитические результаты показывают, что в последовательностях МА для плотного грунта уязвимые нагрузки основного удара-афтершока (MS-AS) являются более разрушительными из-за нагрузки основного удара для всего диаметра. ворса и массы. Для мягкого грунта они более уязвимы к повреждениям из-за основного удара-афтершока (MS-AS). Но в жесткой глине влиянием главного ударно-афтершокового (МС-АС) нагружения по всему диаметру сваи и по массе пренебрегают.

Ключевые слова: мост, взаимодействие грунт-свая-конструкция, фундамент Винклера, динамический расчет, кривые хрупкости, главный толчок-афтершок

1. INTRODUCTION

An earthquake-prone region has the potential to release several extreme earthquake events within a few decades. In one violent earthquake sequence, numerous strong aftershocks occur within several hours or days after the mainshock. For example, On February 6, around 4:15 a.m. local time, a magnitude 7.8 earthquake struck south-central Turkey (Türkiye) near the Turkey/Syria border. Just 11 minutes later, it was followed by a magnitude 6.7 aftershock. The largest aftershock at the time of writing was a M7.5 aftershock which struck 95 km (~60 miles) to the north. USGS observations and analyses indicate all these events are occurring within the East Anatolian fault system.

Bridges are required to withstand a disastrous earthquake without collapses, and retain sufficient capacity along emergency routes prior to/during potential aftershocks in order to promptly dispatch emergency vehicles to the impacted area [2]. In seismically active areas, bridges are subjected to the combined effect of a mainshock (MS) and a series of aftershocks. For example, the March 2011 Tohuku, Japan, earthquake with a moment magnitude (Mw) of 9 was succeeded by hundreds of aftershocks with at least thirty of them greater than Mw 6 [3]. Compared to the MS, the aftershocks (AS) may have significant intensity with a longer effective duration, and different spectral shape, energy content and specific energy density [4].

The diversity of the bridge constitutive components accentuates the need to consider a vast range of interactions, including deck-abutment, abutment embankment [5, 6] and soil-foundation-pier [7, 8] where the Soil-Structure Interaction (SSI) is deemed to represent the most prominent factor in modifying the dynamic response and seismic performance of bridges [9]. Owing to the multi-parametric nature of the soil domain, however, the impact (either favorable or unfavorable) of SSI on the seismic response of bridges is scarce and findings in this domain are conflicting [10]. Until recently, the consensus amongst researchers was that SSI effects are beneficial to the seismic response of bridges by providing a natural isolation layer beneath the bridge with additional flexibility and damping [11]. Mylonakis and Gazetas explored the performance of a simplified bridge-foundation system under a set of actual ground motion records on soft soil and concluded that the elongated period and increased damping of the system has an adverse effect on the imposed seismic demands [9]. In another study, Jeremic et al. conducted a comprehensive finite element analysis on the seismic performance of the I-880 viaduct in California and concluded that depending on the characteristics of the input excitation, SSI can be both beneficial and detrimental [12]. Several other studies have been carried out on the effect of SSI on the seismic response of bridges and shown that SSI has a conspicuous effect on the bridges having relatively light superstructures and heavy substructures regardless of the soil stiffness [10]. The influence of SSI on the seismic performance of the bridge system is a function of the adopted modeling approach of the underlying soil domain. These approaches can be categorized as (a) linear or nonlinear lumped springs at the column bases representing the dynamic characteristics of the of bridge foundations and the supporting soil deposit [13,14]; (b) coupled comprehensive 3D representation of the entire soil-foundation-bridge system [15,16]; and (c) employing the concept of Beam on a Nonlinear Winkler Foundation (BNWF) using a set of distributed dynamic soil springs (p-y, t-z, and q-z) to account for the nonlinear interaction along the length of the piles [17,18]. While the inherent nonlinearity and frequency-dependent nature of the soil is prohibitive in using lumped springs, and the computational cost of analyzing an integrated finite element model of the entire

soil-bridge system is cumbersome, BNWF is discerned to be the most easy-to-manipulate yet accurate approach for simulating the soil domain [17]. Numerous studies have investigated the influence of SSI on the seismic performance of conventionally designed bridges [15;19]. However, there are few publications available in the literature on the extent to which the SSI affects the structural response of seismically isolated bridges [20].

Seismic fragility analysis is a crucial approach to assess the earthquake performance of soil-pile interaction in order to improve the seismic design, retrofitting, and enhancing reliable decision-making on structural engineering. More recently, Ajamy et al.(2018)[21] have worked on an analytical approach to develop seismic fragility curves for an existing Jacket Type Offshore Platforms (JTOP) located in the Persian Gulf using the same data set as described in Ajamy et al. (2014)[22]. The approach used for developing the seismic fragility curves is based on the IDA global interaction method that takes intoaccount the effects of both epistemic and random uncertainties on the expected probability seismic performance of the JTOP. Shafieezadeh et al. (2013)[23] and Su et al. (2017) have used three-dimensional nonlinear FE models to evaluate the seismic performance of dock structures.

Su et al.(2017)[24]have used uncertainties in structural and soil properties as part of a numerical analysis to investigate the variability of seismic behavior of pile-supported wharves.Chara et al. (2016) [25]and Stefanidou et al. (2017) have estimated the effects of SSI on seismic fragility of bridges and building structures respectively. Xiaowei Wang et al.(2019)[26] have identified parameter sensitivity rankings for the evaluation of the seismic performance of bridges supported by groups of piles in liquefiable soils undergoing scour potentials

The primary goal behind the present study is to interrogate the prevailing perception that incorporating the ISSP effects mitigate the probability of damage to a bridge system and its comprising components subjected to mainshock and aftershocks seismic excitations. This research study aims to identify the structural and soil parameters (types of the sand, pile diameter and mass) that have the most and least sensitive effects on theseismic fragility of ISSP system. To reach this objective, a soil-pile-structure finite element (FE) model and a pushover analysis are used to determine the curve of capacity of the ISPS, define the damage condition criteria, and finally generate the fragility curves.

2. NUMERICAL TOOL AND MODELING STRATEGIES

The numerical analyses developed and described in this paper with different nonlinear modeling strategies were studied using the computer program SeismoStruct v7 (SeismoSoft and 2022)[27]. The program includes models for the representation of the behavior of spatial frames and soil under static and/or dynamic loading, considering both material and geometric nonlinearities. With this software, seven types of analyses can be performed, namely: dynamic and static time history (analysis, conventional and adaptive pushover, incremental dynamic analysis, modal analysis, and static analysis (possibly nonlinear) under quasi-permanent loading.

2.1. The Finite Element Model Of Frames

In this study, the elements with distributed inelasticity and all the elements are based on force formulations. In this approach, the entire member is modeled as an inelastic element, the source of such in elasticity beingdefined at the sectional level. The global inelasticity of the frame is obtained by integration of the contribution provided by each controlling section (Fig. 1). A major advantage of such models is the nonexistence of a predetermined length where the inelasticity can occur, because all the sections can have excursions in this field

of response. Though this approach is a closer approximation to reality, it also requires more computational capacity; that is, more analysis time, as well as memory and disk space (Calabrese et al. 2010) [28].

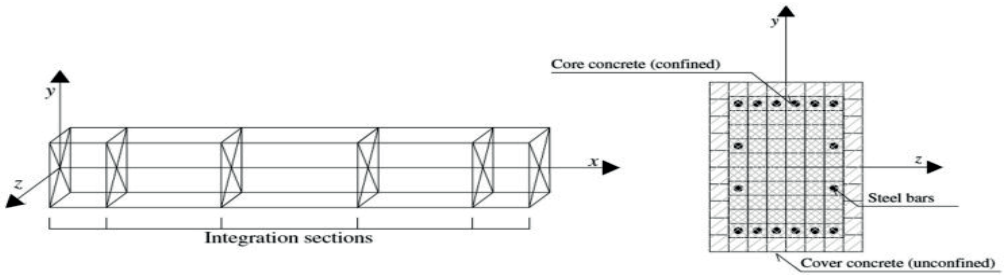


Figure 1. Example of controlling sections along the element and b section fiber discretization

The Material concrete of Mander model was used; to simulate concrete behavior with tensile strength and linear tension softening. For confined concrete material parameters, the equations proposed by Mander et al [29]. were used as represented in Esq.(2) and (3).

$$f_c = K f_c \left[\frac{2\varepsilon_c}{0.002K} - \left(\frac{\varepsilon_c}{0.002K}\right)^2\right]$$

$$K = 1 + \frac{\rho_s f_{\text{yh}}}{f_c}$$

Wherefyhis the hoops yield strength, ρs is the ratio of the volume of hoop reinforcement to the volume of the concrete core, fc, and εc are the concrete longitudinal compressive stress and strain. variable Kf'cand εcu are the ultimate compressive strength and compressive Strain of the confined concrete.

The cyclic behavior of the steel bars is simulated using the classical Menegotto and Pinto (1973) [30]model with kinematic hardening and possibility to take into account buckling by introducing a negative modulus slope in compression depending on the transverse steel reinforcement spacing. The monotonic behavior is defined through the initial Young's modulus (Es), the plastic threshold (esy, rsy), the ultimate strength and strain (eu, ru) and the yielding slope (Eh). The unloading and reloading process, is guided by analytic relations (Eq corresponding to a set of curves ranging between the elastic and the yielding asymptotes

$$\sigma^* = b\varepsilon^* + \left[\frac{1-b}{(1+(\varepsilon^*)^R)^{1/R}}\right]$$

where:

$$\sigma^* = \frac{\sigma_s - \sigma_r}{\sigma_0 + \sigma_r}$$

$$\varepsilon^* = \frac{\varepsilon_s - \varepsilon_r}{\varepsilon_0 + \varepsilon_r}$$

$$R = R_0 - \frac{A_i \xi}{A_j + \xi}$$

Tension: i = 1 and j = 2; Compression: i = 3 and j = 4. (rs, es) is the studied point; (ro, eo) is the crossing point of the elastic and yielding slopes; (rr, er) are the coordinates of the previous point of load reversion; b is the Eh/Es ratio; R is a shape parameter; n is the ratio between the maximum reached strain during loading; eo, Ro, Ai and Aj are material constants that can be obtained from experimental results. A detailed description of the model is presented in Menegotto and Pinto (1928)[31].

2.2. Definiton Ofpy Curves

The backbone curve defined in this model is a multilinear curve defined by fitting a given (theoretical or experimental) non-linear force displacement curve, namely a p-y curve. It is constituted by four segments that can either

simulate monotonic or post-peak behavior (Each slope is determined by the ratio to the initial stiffness of the backbone curve defined by the parameter K0. Cyclic behavior is achieved by introducing specific unload-reload rules. Fig. 2b shows the unloadingcurve, termed the General Unloading Curve (GUC) (segments 5 – 6) and the reloading curve, termed the Standard Reload Curve (SRC) (segments 7 – 8 – 9 – 10), derived by scaling the backbone curve by a factor based on the force at the beginning of reloading or unloading [32] andon the current cyclic degradation factor [33], i.e.

$$\kappa = 1 \pm \frac{p_{ur}}{\delta_s p_f}$$

in which pur is the current force at the onset of unloading or reloading, δs is the strength degradation parameter (described in more detail in the next paragraph) and pf is the ultimate force. The plus (+) and minus (-) signs denote unloading and reloading, respectively. The model simulates either progressive gapping with depth and with the number of load cycles, or pile moving through the slack zone. The Direct Reload Curve (DRC) simulates the soil reaction when the pile moves through the slack zone and is designed as a convex strain-hardening curve controlled by a limiting-force parameter related to the past maximum force. Fig. 2c depicts the formation of pure gap (segment 11), or slack zone (segment 12 characterized by a strain-hardening behavior simulating the densification of the loose caved-in soil).

A generalized fatigue formulation is implemented for simulating the cyclic soil hardening/degradation of both stiffness and strength wheresoil failure conditions and damage evolution functions are dealt separately. The failure condition curve (e.g., S–N curve from cyclic hardening/degradation function [32], used to estimate both the stiffness and strength hardening/degradation factors

$$\delta = 1 + (\delta - 1)\left[1 - (1 - D)^{\theta}\right]^{1/\theta_5}$$

where the subscript ζ stands for either k, the stiffness degradation factor, or s, the strength degradation factor. δ mζ represents the minimum or maximum amount of degradation, D the current cumulative damage and θζ the curve shape parameter. Fig. 3a shows the hardening factor, θζ, versus the number of cycles, N, the maximum hardening factor of δ mζ (> 1) can be achieved by either a concave (θζ< 1) or a linear (θζ =1) or a convex (θζ> 1) curve shape parameter. In Fig. 3b the degradation factor, θζ, versus the number of cycles, N; the minimum degradation factor of δ mζ (< 1) can be attained by either a concave (θζ> 1) or a linear (θζ =1) or a convex (θζ< 1) curve shape parameter. The hardening/degradation factor remains constant as δ mζ is reached. It is worth mentioning that the cyclic soil degradation and hardening is linked to an increase or decrease in the mean effective confining pressure due to the void ratio and pore pressurechanges. The fatigue model used in this paper might be also used for simulating the effects of the liquefaction in terms of degrading behaviour (Allotey and El Naggar[33,34]) but neglects the lateral spreading that can be accounted for by adding further inertial loads tothe pile (e.g. see Brandenburg et al.[35]). In this paper, non-liquefiablesoil deposits are considered.

2.3. Pile-Soil Interaction Analysis With Bnwf

The soil-pile interaction is evaluated using a BNWF model, which approximates the soil-pile interaction using non-linear (p-y) springs in parallel with stiffness proportional dampers. This allows estimating the relative displacements between soil and pile due to the free-field motion. In the BNWF model the pile itself is modelled as a series of beam-column elements, each with discrete springs connecting the pile to the soil, and the freefield motion obtained within the deposit is applied to the p-y springs as excitation to the system.

In this paper, the BNWF model proposed by Allotey and El Naggar[34]is employed for investigating the effect of soil nonlinearity on

the seismic performance of a single pile. This BNWF model is able to simulate generalized dynamic normal force-displacement relationships, accounting for cyclic soil degradation/hardening, soil and structural yielding, slack zone development and radiation damping. In addition, this BNWF model was revised [33] to account for the build-up of pore pressure due to cyclic loading and the different compaction levels of the soil in the vicinity of the pile in a simplified fashion. In particular, a generalized fatigue model based on the total stress method has been developed for simulating cyclic hardening/degradation of stiffness and/ or strength that can account implicitly for several hysteretic soil-pilebehaviours. Finally, results demonstrating the effects of soil non-linearity and the duration of strong motion on the seismic behaviour of piles are compared to the results obtained by the linear soil-pile interaction model defined by Dezi et al. [36,37].

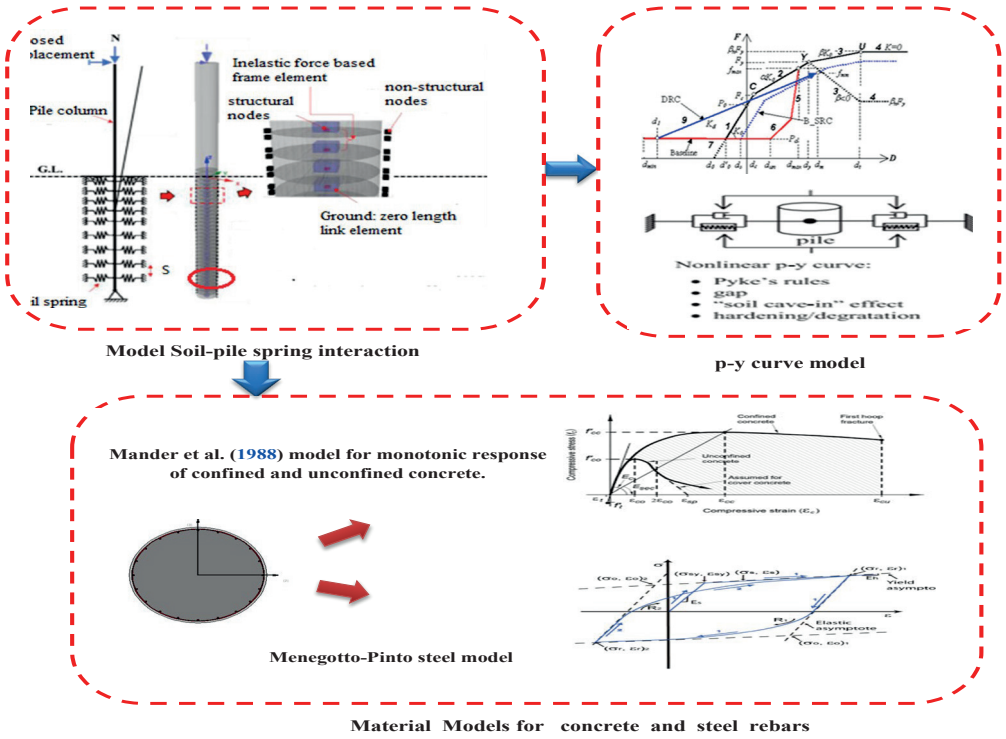


Figure 2. Numerical Tool and Modeling Strategie

3. INCREMENTAL DYNAMIC ANALYSIS AND FRAGILITY ASSESSMENT

IDA is a parametric analysis method that is used to estimate the structural performance under certain earthquake record (see [38]for details). It consists of the development of one curve, under each ground motion, for a specific damage measure (i.e. drift) versus a specific intensity measure of the ground motion (i.e. peak ground acceleration, PGA). The main objectives of IDA are simply to provide deep understanding of the response versus the potential level of the ground motion records and better understanding of the relation of the structural response versus the intensity of the ground motion (maximum displacement, strength, stiffness). This method has been widely used by several researchers in a nonlinear dynamic analysis (see[39;40], for example) as well as in studying pounding phenomenon (see [41-42] for example).

Fragility is the probability of reaching or exceeding a specified damage state. It is expressed in terms of a certain seismic parameter,such as spectral acceleration, spectral

displacement, peak ground velocity and PGA [43-44] Some researchers have provided historical background on the development of the fragility curves (see ,[45-46], forexample). Four different methods can be used to develop the fragility curves, i.e. the expert-based or judgmental method (it depends on the estimates and opinions of experts), empirical method (it is based on thedamage data reported from previous earthquakes - see Ioannou et al.,[47]for example), analytical method (it is based on the time history analyses), andhybrid method (it involves both experimental and numerical analysis [48]). Billah and Alam[49]described the advantages and disadvantages of each method. Among all of them, the analytical method is the most often used one since no experimental or damage datais required for it. One of the most simplest approaches among the analytical methods is the method developed by Ibrahim and El-Shami[50].

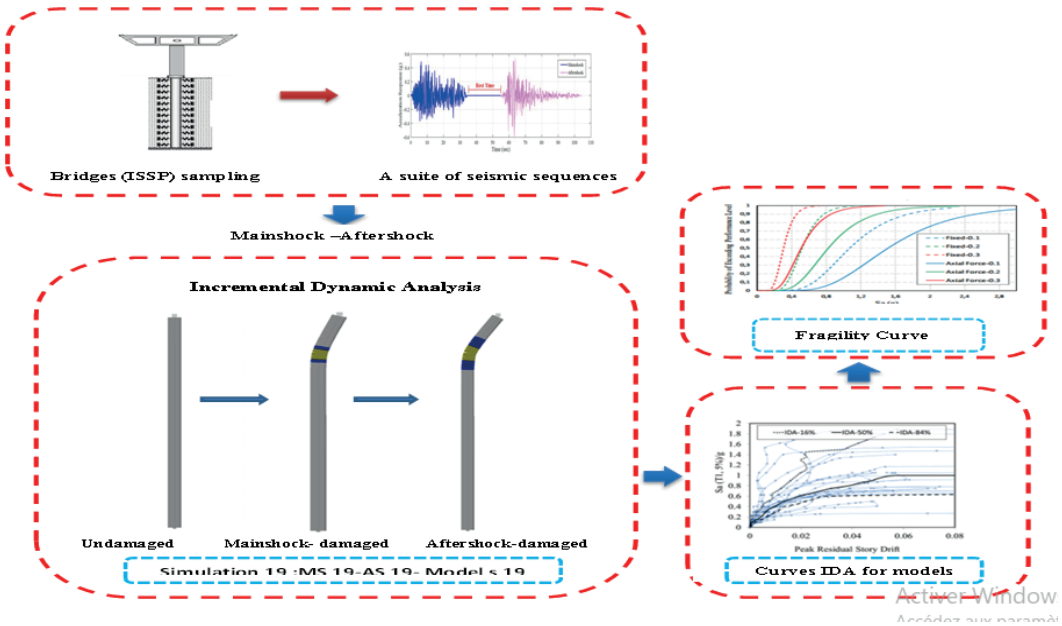


Figure 3. Incremental dynamic analysis method

In this method, the conditional probability of a structure to reach or exceed a specific damage state, D, given the PGA, is defined inEq. (3):

$$P(D/PGA) = \Phi((\ln(PGA) - \mu)/\sigma)$$

whereΦ is the standard normal cumulative distribution function; $\mu$and $\sigma$are the mean value and standard deviation of the natural logarithm of PGA at which the building reaches the threshold of a specific damage state or performance level, D.

Eq. (3) was developed based on the work of Shinozuka et al. [51] where the analytical fragility curves were constructed based on the nonlinear dynamic analysis and the fragility curves were represented by using two-parameter lognormal distribution functions estimated by the maximum likelihood method. The cumulative distribution functions were calculated by dividing the number of data points that reached or exceeded a particular damage state by the number of data points of the whole sample [52]. The accuracy of the use of the mean and standard deviation was investigated and the analytical interpretation of randomness and uncertainty associated with the mean was also provided [51]. Five different damage states/performance levels have been described in the literature, i.e. the operational performance (OP), immediate occupancy (IO), damage control (DC), life safety (LS), and collapse prevention (CP). These

performance levels are defined by certain damage measure, mainly the interstorey drift ratios (or percentages). The maximum allowable interstate drifts for each performance level may differ because it depends on the opinion of the expert. One of the most often used recommendations are the suggestions of Xue et al. [53] which are summarised in Table 1.

Table 1. Limit states considered in this study

Limit state	Transverse drift ratio %
occupancy (IO),	0.7
life safety (LS),	1.5
collapse prevention (CP).	2.5

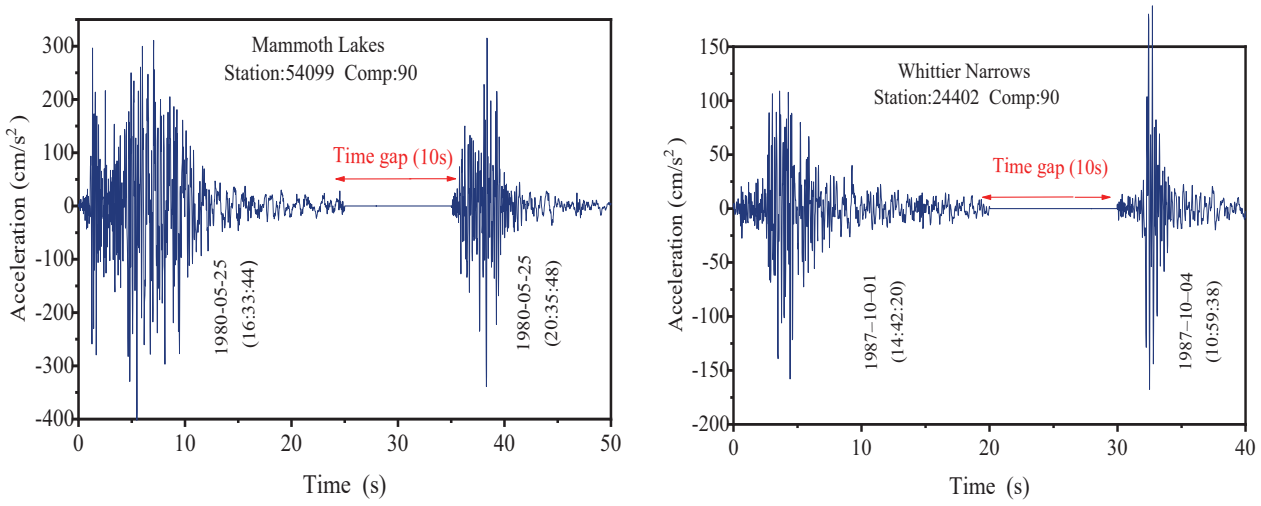
4. GROUND MOTIONS USED IN THE DYNAMIC ANALYSIS

In order to investigate the nonlinear behavior of the mainshockdamaged concrete gravity the ISPS systems for bridge subjected to strong aftershocks, seismic sequences including the mainshock and one major aftershock are needed for performing the nonlinear dynamic analyses. In this study, as-recorded mainshock–aftershock seismic sequences are selected according to the following criteria: (a) the magnitude of the mainshocks isequal to or greater than 5.5 and that of the major aftershocks is equal to or greater than 4.0, (b) accelerograms are recorded at stations, which are located in free fields or low-rise buildings, and (c) the predominant period (Tp) of the mainshocks is less than 0.4 s, which corresponds to the typical dam sites. With these criteria, 19 as-recorded mainshock–- aftershock seismic sequences shown in Table 2, which were recorded at the same station and in the same direction, are selected from the strong motion database of the COSMOS [54]. The data sample includes wellknown earthquakes with strong seismic activities, such as the Mammoth Lakes (1980), Kozani (1995), Whittier Narrows (1987), and Cape Mendocino/Petrolia (1992) events. For each of the 19 sequentialground motion records, the time gap between the mainshock and the aftershock seismic events is set to be 10 s as illustrated in Fig. 4, whichshows the aforementioned four representative mainshock–aftershock seismic sequences. This gap has zero acceleration ordinates and is adequate to allow the structure to cease moving after the previous seismic event.

Table2. List of mainshock-aftershock seismic sequences considered in this investigation

No	Seismicsequences	Station location	Comp.	Date	Mag	R (km)	Recorded PGA (cm/s2)	PredominantPeriod (s)	Duration (5–95%) (s)
1	Mammoth Lake	54099	90	1980-05-25(16:33:44) 1980-05-25 (20:35:48)	6.1(M_L) 5.7(M_L)	9.1 3.4	402.19 338.87	0.22 0.16	8.96 3.54
2	Mammoth Lake	54301	270	1980-05-25(16:33:44) 1980-05-25 (16:49:27)	6.06(M_L) 5.94(M_L)	14.1 14.4	303.97 372.42	0.1 0.25	7.72 3.42
3	ChalfantValley	54428	270	1986–07–21(14:42:26) 1986–07–21(14:51:09)	6.4(M_L) 5.6(M_L)	18.5 27.9	435.80 156.56	0.20 0.12	7.26 7.66
4	ChalfantValley	54428	360	1986–07–21(14:42:26) 1986–07–21(14:51:09)	6.4(M_L) 5.6(M_L)	18.5 27.9	394.60 101.54	0.24 0.12	8.16 11.16

5	ChalfantValley	54171	180	1986–07–21(14:42:26) 986–07–31(07:22:40)	6.4(M_L) 5.6(M_L)	23.7 15.5	249.10 179.66	0.24 0.34	12.76 14.16
6	ChalfantValley	54171	270	1986–07–21(14:42:26) 986–07–31(07:22:40)	6.4(M_L) 5.6(M_L)	23.7 15.5	169.00 121.44	0.36 0.24	17.04 17.18
7	Imperial Valley	0952	140	1979-10-15 (23:16:53) 1979-10-15(23:19:35)	6.5(M_w) 5.01(M_L)	5.2 13.9	539.78 221.36		
8	Imperial Valley	5055	225	1979–10–15(23:16:53) 1979–10–15(23:19:35)	6.5(M_w) 5.01(M_L)	8.8 12.3	242.96 112.67	0.19 0.22	13.32 12.84
9	Imperial Valley	5055	315	1979–10–15(23:16:53) 1979–10–15(23:19:35)	6.5(M_w) 5.01(M_L)	8.8 12.3	209.4 246.96	0.22 0.22	13.22 12.84
10	Kozani	ITSAK	0	1995–05–13(08:47:00) 1995–05–17(04:14:00)	6.1(M_L) 5.3(M_L)	19.5 12.1	211.03 126.19	0.20 0.22	5.84 5.41
11	Kozani	ITSAK	90	1995–05–13(08:47:00) 1995–05–17(04:14:00)	6.1(M_L) 5.3(M_L)	19.5 12.1	136.00 119.26	0.20 0.14	7.72 5.63
12	Whittier Narrows	24400	270	1987–10–01(14:42:20) 1987–10–04(10:59:38)	6.1(M_w) 5.3(M_w)	14.2 16.3	399.10 333.30	0.20 0.14	7.94 5.18
13	Whittier Narrows	24400	360	1987–10–01(14:42:20) 1987–10–04(10:59:38)	6.1(M_w) 5.3(M_w)	14.2 16.3	420.10 308.60	0.18 0.16	7.14 6.2
14	Whittier Narrows	24402	0	1987–10–01(14:42:20) 1987–10–04(10:59:38)	6.1(M_w) 5.3(M_w)	19.4 18..2	299.30 266.00	0.10 0.14	4.54 2.14
15	Whittier Narrows	24402	90	1987–10–01(14:42:20) 1987–10–04(10:59:38)	6.1(M_w) 5.3(M_w)	19.4 18..2	157.90 187.90	0.22 0.14	8.1 3.04
16	Whittier Narrows	24461	270	1987–10–01(14:42:20) 1987–10–04(10:59:38)	6.1(M_w) 5.3(M_w)	13.9 14.8	374.3 210	0.15 0.14	5.72 4.5
17	Northridge	Castaic-Oldridge route	90	1994-01-17 1994-01-17	6.69 5.93		568 138		
18	Northridge	Rinaldi Receiving Sta	318	1994-01-17 1994-03-20	6.69 5.28		472 476		
19	Northridge	0637	270	1994-01-17 1994-01-17	6.69 5.28				



(a) *(b)*

Figure 4. Four representative as-recorded mainshock–aftershock seismic sequence:(a) Mammoth Lakes, Station: 54099-Comp;(b) WhittierNarrows, Station: 24402-Comp

5. NUMERICAL MODELS OF BUILDINGS

Figure 5 shows a single column that extend to5m above and 30m below ground. The column has a uniform section and steel reinforcement. SeismoStruct v7 (SeismoSoft and 2022) software allows for strength and stiffness degradation in the components by providing the force deformation criteria for hinges used in the numerical analyses. The material properties of the structure, piles and soils are given in Tables 3and 4

Table 3. The problem investigated and the two types of presumed soil deposits

	Loose sand φ=30°	Dense sand φ=45°	Soft clay	Stiff clay
Kpy (below water table) (MN/m3)	5.4	12.66	0.5	30.

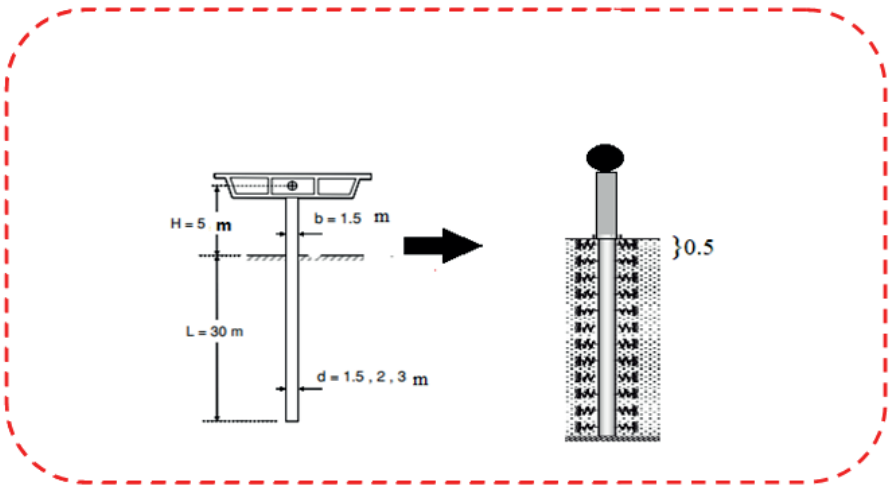


Figure 5. Interaction of soil-pile-structure configuration

Table 4. Parametric cases

Parameter	M(t)	Pile diameter, D (m)	Type of soil
Value	**150;350; 700**	**1.5 ; 2 ;3**	**(Loose,Dense)sand (soft,stiff) clay**

5.1. Pushover Results

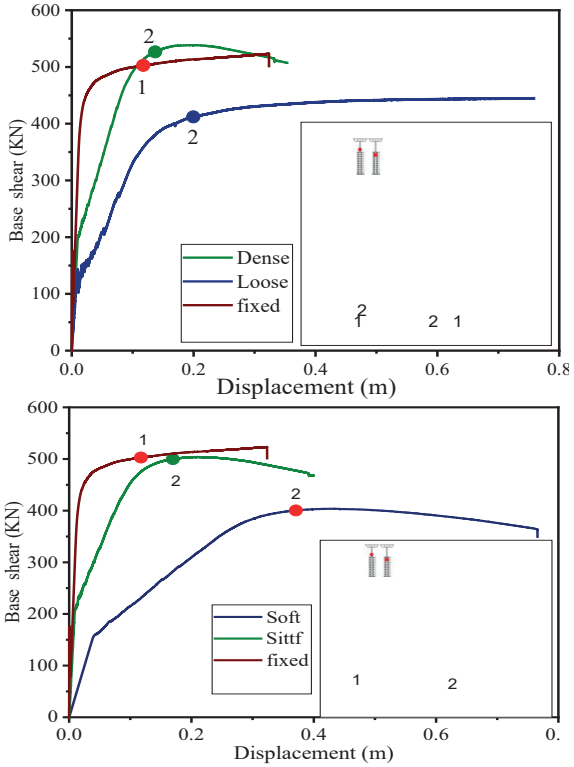


Figure 6. Lateral load-Displacement behaviour: the ISPS system and the fixed: a) sand; b) clay

Figure 6 show Lateral load-Displacement behaviour the ISPS system: a) sand; b) clay The results indicate that the lateral capacity of the dense sand more capacity and less ductility compared the loose sand and the fixed ,note in the result the lateral capacity of the soft caly gives a lower lateral capacity and more ductility compared the stiff clay

5.2. Ida Results

The figure 7 presented the IDA results obtained with nonlinearanalysis of 19 earthquakes for the two extreme cases (mainshock only and mainshock - aftershock) for ISPS system with dens soil type. In order to show the effect of earthquakes with the two extreme cases, after the end of IDA analysis, we take the average results of the acceleration for each displacement.

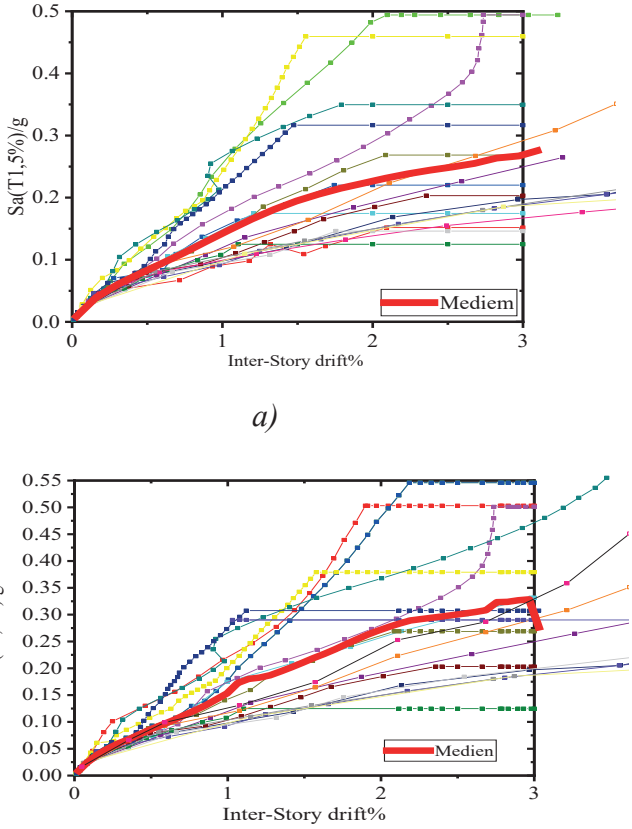
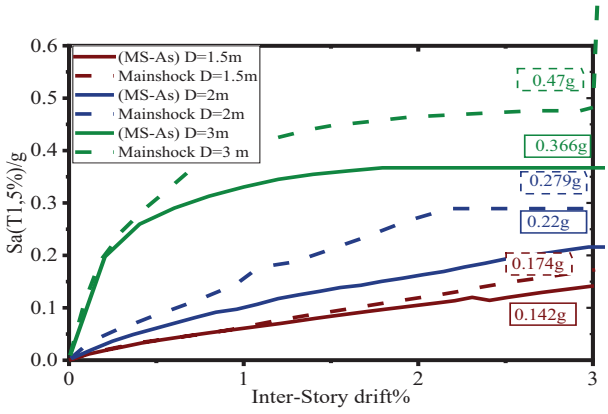


Figure 7. IDA results in ISPS system (a) Mainshock+Aftershock; (b) Mainshock

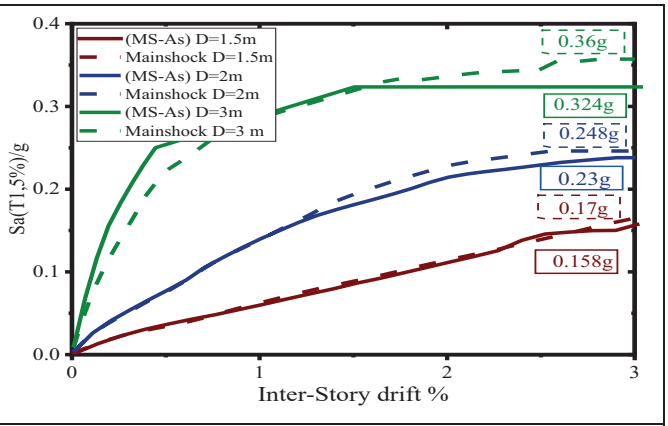
Effects of the Section of Pile

The average IDA curves for the ISPS systems for dense soil and Losse soil are presented in the Figs 8 The results indicated that the effect of the aftershock damage on ISPS are negative and depend on the diameter of the pile. For the dense soil, the results show the decrease in the values of acceleration after adding the aftershock earthquake with the percentage

18.3%, 21.5% and 23.04% for diameters 1.5m, 2m and 3m respectively. For the losses soil, the results show the slight decrease in the values of acceleration after adding the aftershock earthquake with the percentage 7.01%, 8.26% and 10.04% for diameters 1.5m, 2m and 3m respectively.

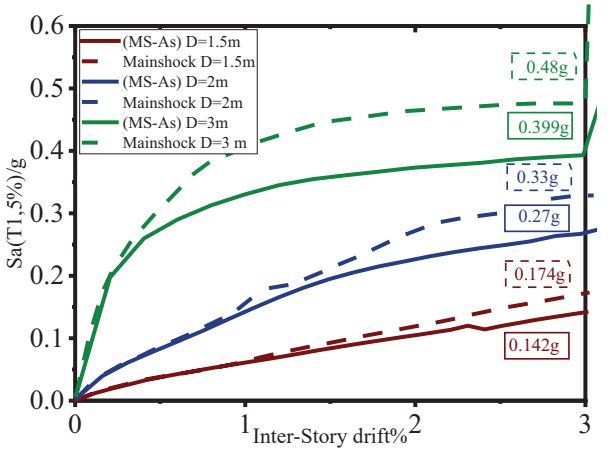


(a)Dense

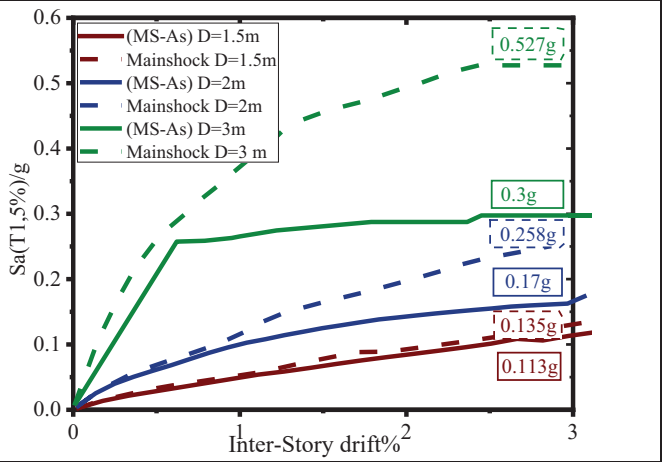


(b) Loose

Figure 8. Average IDA curves of in ISPS system different section :Mainshock+Aftershock; and Mainshock for Dense soil and Losse soil



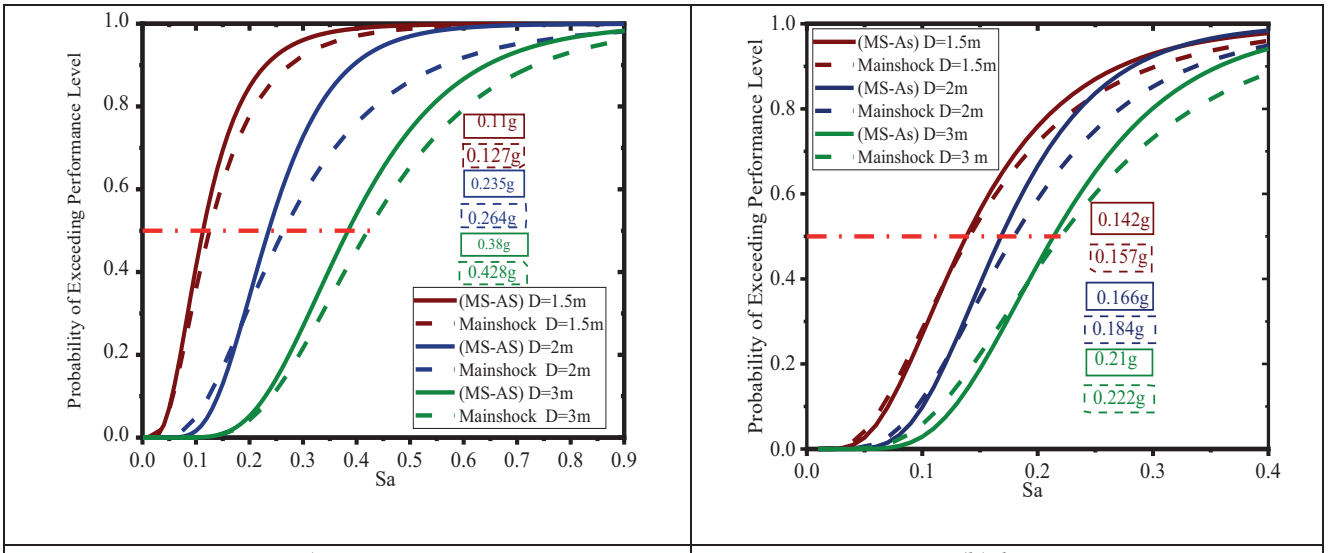
a) Soft



b) Stiff

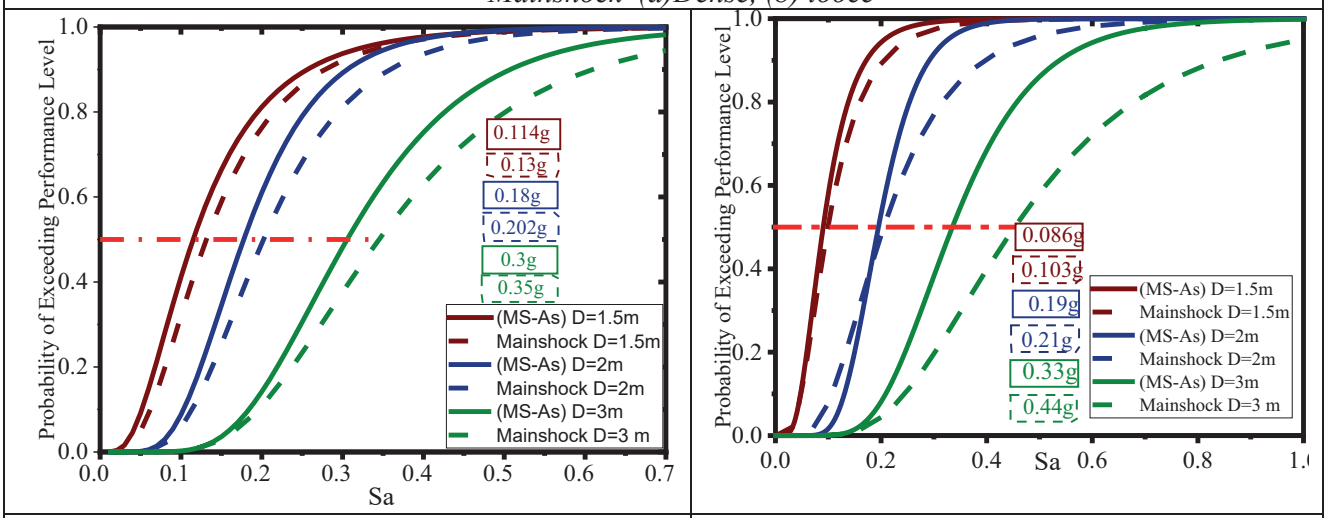
Figure 9. Average IDA curves of in ISPS system different section :Mainshock+Aftershock; and Mainshock for Soft and Stiff soils

Figure 9 The average IDA results forISPS systems for soft soil and stiff! soil shows that the consideration of aftershocks The influence can be seen in the differences between the median curves;increases the extent of ISPS systems responses and depend on the diameter of the pile; For the soft soil, the results show the decrease in the values of acceleration after adding the aftershock earthquake with the percentage 12.2%, 15.77% and 23.5% for diameters 1.5m, 2m and 3m respectively. For the stiff soil, the results show the decrease in the values of acceleration after adding the aftershock earthquake with the percentage 16.3%, 34.1% and 43.64% for diameters 1.5m, 2m and 3m respectively



a) Dense *(b) loose*

Figure 10. Fragility curves of theSPS system different section :Mainshock+Aftershock; and Mainshock (a)Dense, (b) looce



(a) Soft *(b) stiff*

Figure 11. Fragility curves of theSPS system different section :Mainshock+Aftershock; and Mainshock (a) Soft, (b) Stiff.

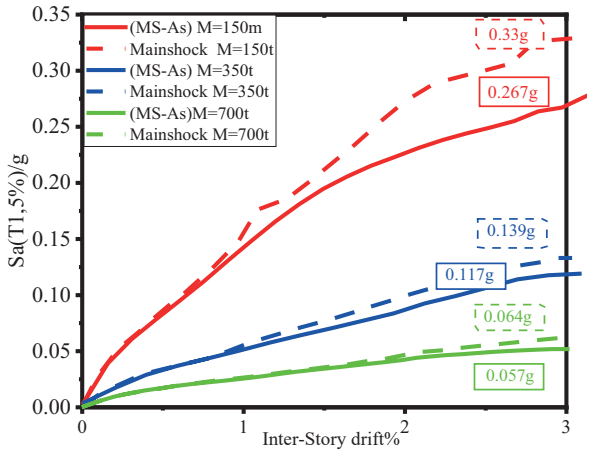
Figure 10 and 11 show the fragility curve under loading of Mainshock+Aftershock and Mainshock with variation of the pile section for Dense, loose, soft and stiff soil.For the probability of exceeding equal to 50%, when add aftershock and increase in the diameter of pile the damage state becomes more serious,for the dense sand the medium intensity S_{ct} are increased with 0.017g, 0.029g, 0.04g for 1.5 m, 2 m and 3 m diameters, respectively. As in the loose sand Sct are increased with 0.015g, 0.018g, 0.0212g for 1.5 m, 2 m and 3 m diameters, respectively. As for the soft caly are increased with 0.016g, 0.022g, 0.05g for 1.5 m, 2 m and 3 m diameters, respectively.

And for stiff clay the medium intensity Sct are increased with 0.017g, 0.02g, 0.11g for 1.5 m, 2 m and 3 m diameters, respectively.

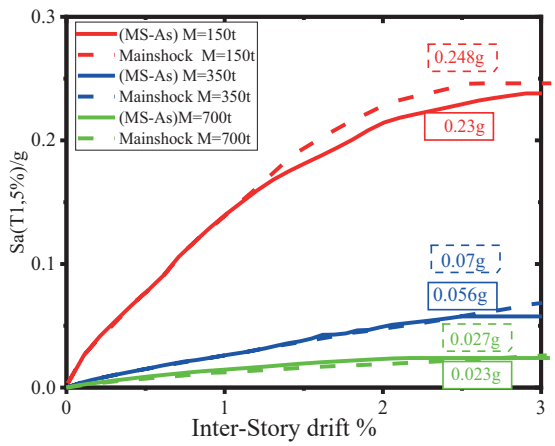
Effects of the mass

Fig. 12 shows the average IDA curves for ISPS systems for different types of sand (dense sand loose sand) under mainshock-only and the mainshock-aftershock loading with the varying of the masse (150t , 350t ,700t). Can be seen that the effect of the mainshock-aftershock loading are neglected when the inter-story drift as low as to 1%, but when the inter-story drift grate to 1% the effect it depends on sand types and masse.

For dense sand the results gives a decrease with 10.33% .15.83% and 18.57% for masse 150t, 350t and 700t respectively, and for loose sand with masse 150t the results give a decrease with 7.26% but for masse 350t and 700t the effect of aftershockare neglected.



(a)Dense



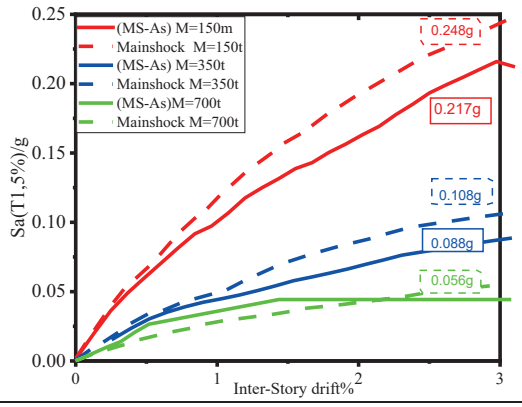
(b) Loose

Figure 12. Average IDA curves of in ISPS system different mass :Mainshock+Aftershock; and Mainshock: (a)Dens (b)Loose

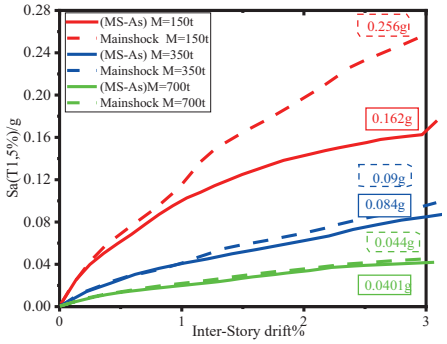
Fig. 12 shows the average IDA curves for ISPS systems for different types of clay (soft clay stiff clay) under mainshock-only and the mainshock-aftershock loading with the varying of the masse (150t , 350t ,700t). Can be seen that the effect of the mainshock-aftershock loading are neglected when the inter-story drift as low as to 1%, but when the inter-story drift grate to 1% the effect it depends on sand types and masse.

For soft clay the results gives a decrease with 12.5% 22.7% and for masse 150t, 350t and and 700t the effect of aftershockare neglected, and for stiff clay with masse 150t the results give a decrease with 36.7% but for masse 350t and 700t the effect of aftershockare neglected.

For the dense sand, the medium intensity S_{ct} are increased with 0.029g, 0.014g, 0.008g for 150t, 350t and 700t masse, respectively. As in the loose sand Sct are increased with 0.027g, 0.013g, 0.009g for 150t, 350t and 700t mass, respectively. As for the soft caly are increased with 0.022g, 0.017g, 0.015g for for 150t, 350tand 700t masse, respectively. And for stiff clay the medium intensity S_{ct} are increased with 0.012g, 0.009g, 0.008g for 150t, 350tand 700t masse respectively.In globale the results indicat that the efect of the masse and type of soil are effected by mainshock-aftershock.

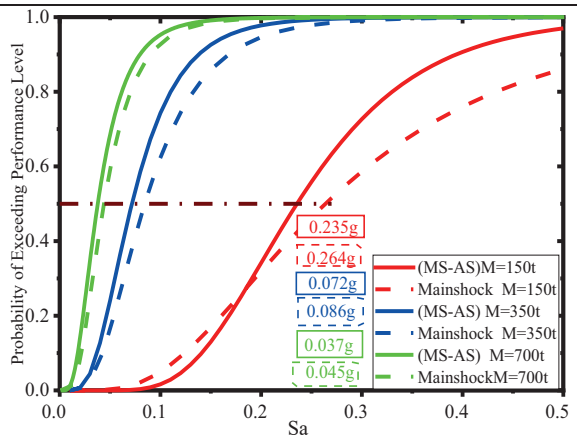


(a) Soft

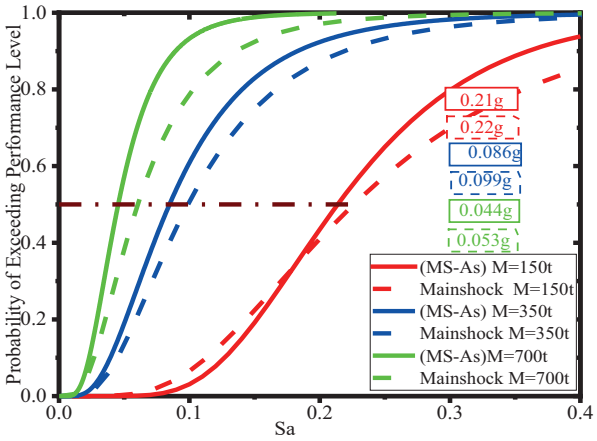


(b)Stiff

Figure 13. Average IDA curves of in ISPS system different mass :Mainshock+Aftershock; and Mainshock: (a) Soft ;(b)stiff

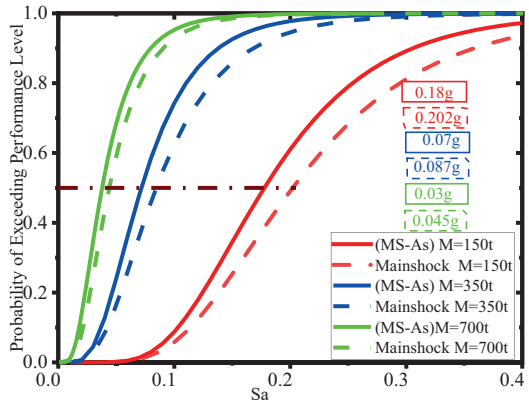


(a)Dense

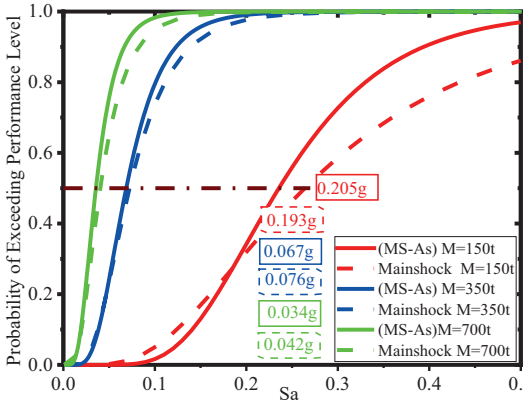


(b) Loose

Figure 14. Fragility curves of the ISPS system different mass :Mainshock+Aftershock; and Mainshock: (a) Denes; (b) Loose



(a)Soft



(b) stiff

Figure 15. Fragility curves of the ISPS system different mass :Mainshock+Aftershock; and Mainshock: (a) Soft; (b) Stiff

CONCLUSION

In this paper, the seismic evaluation of soil structure system (ISPS) with different soil, diameter and mass , subjected to sequential mainshock-aftershock records, was studied by means of the pushover analysis and IDA for generate the fragility curves. The effect of the soil type, masse, diametre of pile on ISPS system under mainshock (MS) and mainshock-aftershock (MS-AS) loading was investigated in this paper using the pushover, the IDA and the fragility assessment methods. Four type of soils (dense and loose sand, soft and stiff caly) with different masse (150t, 350t, 700t) and varing the diamtre of pile (1.5m, 2m, 3m) were considered in the study.From the findings of this research, the following conclusions can be drawn:

- In most cases, the lateral capacity of the loose gives a lower lateral capacity to dense sand, but about the ductility the loose sand more ductility. And for clay, the stiff clay show higher lateral capacity to soft clay.
- Based on both IDA and fragility assessment methods, the effect of type soil on ISPS system : for dense soil the vulnerable of mainshock-aftershock (MS-AS) loading are more damage due to mainshock loading for all diameter of the pile and the masse; But for loose sand the effect of aftershock are neglected after mainshock loading for all the diameter of the pile and the masse effect.
- The effect of clay type on ISPS system : for soft soil are more vulnerable to damage due to mainshock-aftershock (MS-AS) loading. but in the stiff clay the effect of mainshock-aftershock (MS-AS) loading for all the diameter of pile and for masse are neglected.

REFERENCE

1. **C.E. Administration,** Earthquake Site Work Outline and Technical Guidelines, Earthquake press, Beijing, 1998
2. **Chang L, Peng F, Ouyang Y, Elnashai AS, Spencer Jr BF.** Bridge seismicretrofit program planning to maximize postearthquake transportation networkcapacity. J Inf Syst 2012;18(2):75–88. http://dx.doi.org/10.1061/(ASCE)IS.1943-555X.0000082.
3. USGS, United states geological survey, 2012. <http://www.usgs.gov/>
4. **Li Y, Song R, Van De Lindt JW.** Collapse fragility of steel structures subjected to earthquake mainshock–aftershock sequences. J Struct Eng 2014.http://dx.doi.org/10.1061/(ASCE)ST.1943-541X.0001019
5. **Zhang J, Makris N.** Kinematic response functions and dynamic stiffnesses of bridgeembankments. Earthq Eng Struct Dynam 2002;31:1933–66
6. **Kotsoglou A, Pantazopoulou S**. Bridge–embankment interaction under transverse ground excitation. Earthq Eng Struct Dynam 2007;36:1719–40.
7. **Mylonakis G, Nikolaou S, Gazetas G.** Footings under seismic loading: analysis anddesign issues with emphasis on bridge foundations. Soil DynamEarthqEng2006;26:824–53.
8. **Elgamal A, Yan L, Yang Z, Conte JP.** Three-dimensional seismic response ofHumboldt Bay bridge-foundation-ground system. J Struct Eng 2008;134:1165–76.
9. **Mylonakis G, Gazetas G.** Seismic soil-structure interaction: beneficial ordetrimental? J Earthq Eng 2000/07/01 2000;4:277–301.
10. **Stefanidou SP, Sextos AG, Kotsoglou AN, Lesgidis N, Kappos AJ.** Soil-structureinteraction effects in analysis of seismic fragility of bridges using an intensity-basedground motion selection procedure. Eng Struct 2017;151:366–80.
11. **Ucak A, Tsopelas P**. Effect of soil–structure interaction on seismic isolated bridges.J Struct Eng 2008;134:1154–64.
12. **Jeremi´c B, Kunnath S, Xiong F.** Influence of soil–foundation–structure interactionon seismic response of the I-880

viaduct. Eng Struct 2004/02/01/2004;26:391–402.
13. **Xiang N, Alam MS.** Comparative seismic fragility assessment of an existing isolatedcontinuous bridge retrofitted with different energy dissipation devices. J BridgeEng 2019;24:04019070.L. Su, H.-P. Wan, Y. Dong, D. M. Frangopol, and .
14. **Yang C-SW, Werner SD, DesRoches R.** Seismic fragility analysis of skewed bridges in the central southeastern United States. Eng Struct 2015/01/15/2015;83: 116–28.
15. **Rahmani A, Taiebat M, Liam Finn WD, Ventura CE.** Evaluation of substructuring method for seismic soil-structure interaction analysis of bridges. Soil Dynam Earthq Eng 2016/11/01/2016;90:112–27.
16. **Xie Y, DesRoches R.** Sensitivity of seismic demands and fragility estimates of a typical California highway bridge to uncertainties in its soil-structure interactio modeling. Eng Struct 2019/06/15/2019;189:605–1
17. **Noori HR, Memarpour MM, Yakhchalian M, Soltanieh S.** Effects of ground motion directionality on seismic behavior of skewed bridges considering SSI. Soil Dynam Earthq Eng 2019/12/01/2019;127:105820.
18. **Mallick M, Raychowdhury P.** Seismic analysis of highway skew bridges with nonlinear soil–pile interaction. Transport Geotech 2015/06/01/2015;3:36–47.
19. **Carbonari S, Morici M, Dezi F, Gara F, Leoni G.** Soil-structure interaction effects in single bridge piers founded on inclined pile groups. Soil Dynam Earthq Eng 2017/01/01/2017;92:52–67.
20. **Gonz´ alez F, Padron ´ LA, Carbonari S, Morici M, Aznarez ´ JJ, Dezi F, et al.** Seismicresponse of bridge piers on pile groups for different soil damping models and lumped parameter representations of the foundation. Earthq Eng Struct Dynam 2019;48:306–27.
21. **Vlassis A, Spyrakos C.** Seismically isolated bridge piers on shallow soil stratum with soil–structure interaction. Comput Struct 2001;79:2847–61.
22. **Ajamy, A., Asgarian, B., Ventura, C.E., Zolfaghari, M.R.:** Seismic fragility analysis of jacket type offshoreplatforms considering soil-pile-structure interaction. Eng. Struct. 174, 198–211 (2018). https://doi.org/10.1016/j.engstruct.2018.07.066
23. **Ajamy, A., Zolfaghari, M.R., Asgarian, B., Ventura, C.E.:** Probabilistic seismic analysis of offshore platformsincorporating uncertainty in soil–pile–structure interactions. J. Constr. SteelRes. 101, 265–279 (2014). https://doi.org/10.1016/j.jcsr.2014.05.024
24. **Shafieezadeh, A., DesRoches, R., Rix, G.J., Werner, S.D.**: Three-dimensional wharf response to far-field andimpulsive near-field ground motions in liquefiable soils. J. Struct. Eng. 139(8), 1395–1407 (2013). https://doi.org/10.1061/(asce)st.1943-541x.0000642
25. **Stefanidou, S.P., Sextos, A.G., Kotsoglou, A.N., Lesgidis, N., Kappos, A.J.:** Soil-structure interaction effectsin analysis of seismic fragility of bridges using an intensity-based ground motion selection procedure. Eng. Struct. 151, 366–380 (2017). https://doi.org/10.1016/j.engstruct.2017.08.033
26. **Chara, C., Mitropoulou, C.C., Kostopanagiotis, C., Kopanos, M., Ioakim, D., Lagaros, N.D.:** Influence of soilstructure interaction on fragility assessment of building structures. In: Structures, pp. 85–98. Elsevier (2016). https://doi.org/10.1016/j.istruc.2016.02.005
27. **Wang, X., Ye, A., Ji, B.:** Fragility-based sensitivity analysis on the seismic performance of pile-group supported bridges in liquefiable ground undergoing scour potentials. Eng. Struct. 198, 109427 (2019). https://doi.org/10.1016/j.engstruct.2019.109427 program SeismoStruct v7 (SeismoSoft and 2022)

28. **Calabrese, A., Almeida, J. P., & Pinho, R.** (2010). Numericalissues in distributed inelasticity modeling of RC frameelements for seismic analysis. Journal of EarthquakeEngineering, 14(S1), 38–68.
29. **Menegotto, M., & Pinto, P.E.** (1973). Method of analysis forcyclically loaded reinforced concrete plane frames including changes in geometry and non-elastic behavior of elements under combined normal force and bending moment(pp. 15–22). Lisbon, Portugal: IASBE Proceedings
30. **Mander JB, Priestley MJN, Park R.** Theoretical stress-strain model for confinedconcrete. Struct Eng 1998;114(8):1804–26
31. **Richart, F.E., Brandtzæg, A., & Brown, R.** L. (1928). A studyof the failure of concrete under combined compressive stresses. University of Illinois Bulletin, 26(12)
32. **Pyke RM.** Nonlinear soil models for irregular cyclic loadings. J Geotech Eng Div,ASCE 1979;105(6):715–26
33. **Allotey N, Naggar MH El.** A consistent soil fatigue framework based on the number of equivalent cycles. Geotech Geol Eng 2007;26(1):65–77.
34. **Allotey N, Naggar MH E**l. Generalized dynamic Winkler model for nonlinear soil–structure interaction analysis. Can Geotech J 2008;45(4):560–73
35. **Brandenberg SJ, Boulanger RW, Kutter BL, Chang D**. Behavior of pile foundations inlaterally spreading ground during centrifuge tests. J Geotech Geoenviron Eng2005;131(11):1378–91.
36. **Dezi F, Carbonari S, Leoni G.** A model for the 3D kinematic interaction analysis ofpile groups in layered soils. Earthq Eng Struct Dyn 2009;38(11):1281–305
37. **Dezi F, Carbonari S, Morici M.** A numerical model for the dynamic analysis of inclined pile groups: a numerical model for the dynamic analysis of inclined pile groups. Earthq Eng Struct Dyn 2016;45(1):45–68.
38. **Vamvatsikos Dimitrios, Cornell C Allin**. Incremental dynamic analysis. EarthquakeEng Struct Dyn 2002;31(3):491–514
39. **Mander JB, Dhakal RP, Mashiko N, Solberg KM**. Incremental dynamic analysis applied to seismic financial risk assessment of bridges. Eng Struct2007;29(10):2662–7
40. **Chomchuen Prakit, Boonyapinyo Virote.** Incremental dynamic analysis with multimodes for seismic performance evaluation of RC bridges. Eng Struct2017;132:29–43
41. **Kazemi F, Mohebi B, Yakhchalian M.** Evaluation of the P-delta effect oncollapsecapacity of adjacent structures subjected to far-field ground motions.CivilEngJ2018;4(5):1066–73.
42. performance ofadjacent pounding structures using viscous dampers. In: The16thEuropeanConference on Earthquake Engineering; 2018. p. 18–21
43. **Kostov M.** Seismic fragility analyses. In "Regional Workshop On ExternalEventsPSA 6-10 November 2000, Sofia," 2000
44. **Duan X, Pappin JW.** "A procedure for establishing fragility functions for seismicloss estimate of existing buildings based on nonlinear pushover analysis,"in14thWorld Conference on Earthquake Engineering. Beijing: China; 2008. p. 12–7
45. **Kumitani S, Takada T.** Probabilistic assessment of buildings damage consideringaftershocks of earthquakes. 14th World Conference on EarthquakeEngineering.2008.
46. **Haran Pragalath DC, Davis R, Sarkar P.** Reliability evaluation of RC framebytwomajor fragility analysis methods. Asian J. Civil Eng. (BuildingAndHousing)2015;16:47–66.
47. Ioannou Ioanna, Douglas John, Rossetto Tiziana. Assessing the impact of groundmotion variability and uncertainty on empirical fragility

curves.SoilDynEarthquake Eng 2015;69:83–92.
48. **Kappos Andreas J, Panagopoulos Georgios, Panagiotopoulos Christos, Penelis Gregorios.** A hybrid method for the vulnerability assessment of R/CandURM buildings. Bull Earthq Eng 2006;4(4):391–413.
49. **Muntasir Billah AHM, Shahria Alam M.** Seismic fragility assessment of highway bridges: a state-of-the-art review. Struct Infrastruct Eng 2015;11(6):804–32.
50. **Ibrahim Yasser E, El-Shami Mostafa M.** Seismic fragility curves for mid-risereinforced concrete frames in Kingdom of Saudi Arabia. IES J PartA:CivilStructEng 2011;4(4):213–23.
51. **Shinozuka M, Feng MQ, Kim H-K, Kim S-H.** Nonlinear static procedurefor + fragilitycurve development. JEngMech 2000; 126 (12):1287–95.
52. **Shinozuka M, Feng M, Kim H, Uzawa T, Ueda T.** "Statistical analysis offragilitycurves. Technical Report." Multidisciplinary Center for Earthquake Engineering Research, MCEER-032003.
53. **Xue Q, Wu C-W, Chen C-C, Chen K-C.** The draft code for performance-based seismic design of buildings in Taiwan. Eng Struct 2008;30(6):1535–47.
54. COSMOSVirtualDataCenter.:⟨http://strong motioncenter.org/vdc/scripts/de

СПИСОК ЛИТЕРАТУРЫ

1. **C.E. Administration,** Earthquake Site Work Outline and Technical Guidelines, Earthquake press, Beijing, 1998
2. **Chang L, Peng F, Ouyang Y, Elnashai AS, Spencer Jr BF.** Bridge seismicretrofit program planning to maximize postearthquake transportation networkcapacity. J Inf Syst 2012;18(2):75–88. http://dx.doi.org/10.1061/(ASCE)IS.1943-555X.0000082.
3. USGS, United states geological survey, 2012. <http://www.usgs.gov/>
4. **Li Y, Song R, Van De Lindt JW.** Collapse fragility of steel structures subjected to earthquake mainshock–aftershock sequences. J Struct Eng 2014.http://dx.doi.org/10.1061/(ASCE)ST.1943-541X.0001019
5. **Zhang J, Makris N.** Kinematic response functions and dynamic stiffnesses of bridgeembankments. Earthq Eng Struct Dynam 2002;31:1933–66
6. **Kotsoglou A, Pantazopoulou S**. Bridge–embankment interaction under transverse ground excitation. Earthq Eng Struct Dynam 2007;36:1719–40.
7. **Mylonakis G, Nikolaou S, Gazetas G.** Footings under seismic loading: analysis anddesign issues with emphasis on bridge foundations. Soil DynamEarthqEng2006;26:824–53.
8. **Elgamal A, Yan L, Yang Z, Conte JP.** Three-dimensional seismic response ofHumboldt Bay bridge-foundation-ground system. J Struct Eng 2008;134:1165–76.
9. **Mylonakis G, Gazetas G.** Seismic soil-structure interaction: beneficial ordetrimental? J Earthq Eng 2000/07/01 2000;4:277–301.
10. **Stefanidou SP, Sextos AG, Kotsoglou AN, Lesgidis N, Kappos AJ.** Soil-structureinteraction effects in analysis of seismic fragility of bridges using an intensity-basedground motion selection procedure. Eng Struct 2017;151:366–80.
11. **Ucak A, Tsopelas P**. Effect of soil–structure interaction on seismic isolated bridges.J Struct Eng 2008;134:1154–64.
12. **Jeremi´c B, Kunnath S, Xiong F.** Influence of soil–foundation–structure interactionon seismic response of the I-880 viaduct. Eng Struct 2004/02/01/2004;26:391–402.
13. **Xiang N, Alam MS.** Comparative seismic fragility assessment of an existing isolatedcontinuous bridge retrofitted with different energy dissipation devices. J

BridgeEng 2019;24:04019070.L. Su, H.-P. Wan, Y. Dong, D. M. Frangopol, and .

14. **Yang C-SW, Werner SD, DesRoches R.** Seismic fragility analysis of skewed bridges in the central southeastern United States. Eng Struct 2015/01/15/2015;83: 116–28.
15. **Rahmani A, Taiebat M, Liam Finn WD, Ventura CE.** Evaluation of substructuring method for seismic soil-structure interaction analysis of bridges. Soil Dynam Earthq Eng 2016/11/01/2016;90:112–27.
16. **Xie Y, DesRoches R.** Sensitivity of seismic demands and fragility estimates of a typical California highway bridge to uncertainties in its soil-structure interactio modeling. Eng Struct 2019/06/15/2019;189:605–1
17. **Noori HR, Memarpour MM, Yakhchalian M, Soltanieh S.** Effects of ground motion directionality on seismic behavior of skewed bridges considering SSI. Soil Dynam Earthq Eng 2019/12/01/2019;127:105820.
18. **Mallick M, Raychowdhury P.** Seismic analysis of highway skew bridges with nonlinear soil–pile interaction. Transport Geotech 2015/06/01/2015;3:36–47.
19. **Carbonari S, Morici M, Dezi F, Gara F, Leoni G.** Soil-structure interaction effects in single bridge piers founded on inclined pile groups. Soil Dynam Earthq Eng 2017/01/01/2017;92:52–67.
20. **Gonz´ alez F, Padron ´ LA, Carbonari S, Morici M, Aznarez ´ JJ, Dezi F, et al.** Seismicresponse of bridge piers on pile groups for different soil damping models and lumped parameter representations of the foundation. Earthq Eng Struct Dynam 2019;48:306–27.
21. **Vlassis A, Spyrakos C.** Seismically isolated bridge piers on shallow soil stratum with soil–structure interaction. Comput Struct 2001;79:2847–61.
22. **Ajamy, A., Asgarian, B., Ventura, C.E., Zolfaghari, M.R.:** Seismic fragility analysis of jacket type offshoreplatforms considering soil-pile-structure interaction. Eng. Struct. 174, 198–211 (2018). https://doi.org/10.1016/j.engstruct.2018.07.066
23. **Ajamy, A., Zolfaghari, M.R., Asgarian, B., Ventura, C.E.:** Probabilistic seismic analysis of offshore platformsincorporating uncertainty in soil–pile–structure interactions. J. Constr. SteelRes. 101, 265–279 (2014). https://doi.org/10.1016/j.jcsr.2014.05.024
24. **Shafieezadeh, A., DesRoches, R., Rix, G.J., Werner, S.D.**: Three-dimensional wharf response to far-field andimpulsive near-field ground motions in liquefiable soils. J. Struct. Eng. 139(8), 1395–1407 (2013). https://doi.org/10.1061/(asce)st.1943-541x.0000642
25. **Stefanidou, S.P., Sextos, A.G., Kotsoglou, A.N., Lesgidis, N., Kappos, A.J.:** Soil-structure interaction effectsin analysis of seismic fragility of bridges using an intensity-based ground motion selection procedure. Eng. Struct. 151, 366–380 (2017). https://doi.org/10.1016/j.engstruct.2017.08.033
26. **Chara, C., Mitropoulou, C.C., Kostopanagiotis, C., Kopanos, M., Ioakim, D., Lagaros, N.D.:** Influence of soilstructure interaction on fragility assessment of building structures. In: Structures, pp. 85–98. Elsevier (2016). https://doi.org/10.1016/j.istruc.2016.02.005
27. **Wang, X., Ye, A., Ji, B.:** Fragility-based sensitivity analysis on the seismic performance of pile-group supported bridges in liquefiable ground undergoing scour potentials. Eng. Struct. 198, 109427 (2019). https://doi.org/10.1016/j.engstruct.2019.109427 program SeismoStruct v7 (SeismoSoft and 2022)
28. **Calabrese, A., Almeida, J. P., & Pinho, R.** (2010). Numericalissues in distributed inelasticity modeling of RC frameelements for seismic analysis. Journal of EarthquakeEngineering, 14(S1), 38–68.

29. **Menegotto, M., & Pinto, P.E.** (1973). Method of analysis forcyclically loaded reinforced concrete plane frames including changes in geometry and non-elastic behavior of elements under combined normal force and bending moment(pp. 15–22). Lisbon, Portugal: IASBE Proceedings
30. **Mander JB, Priestley MJN, Park R.** Theoretical stress-strain model for confinedconcrete. Struct Eng 1998;114(8):1804–26
31. **Richart, F.E., Brandtzæg, A., & Brown, R.** L. (1928). A studyof the failure of concrete under combined compressive stresses. University of Illinois Bulletin, 26(12)
32. **Pyke RM.** Nonlinear soil models for irregular cyclic loadings. J Geotech Eng Div,ASCE 1979;105(6):715–26
33. **Allotey N, Naggar MH El.** A consistent soil fatigue framework based on the number of equivalent cycles. Geotech Geol Eng 2007;26(1):65–77.
34. **Allotey N, Naggar MH E**l. Generalized dynamic Winkler model for nonlinear soil–structure interaction analysis. Can Geotech J 2008;45(4):560–73
35. **Brandenberg SJ, Boulanger RW, Kutter BL, Chang D**. Behavior of pile foundations inlaterally spreading ground during centrifuge tests. J Geotech Geoenviron Eng2005;131(11):1378–91.
36. **Dezi F, Carbonari S, Leoni G.** A model for the 3D kinematic interaction analysis ofpile groups in layered soils. Earthq Eng Struct Dyn 2009;38(11):1281–305
37. **Dezi F, Carbonari S, Morici M.** A numerical model for the dynamic analysis of inclined pile groups: a numerical model for the dynamic analysis of inclined pile groups. Earthq Eng Struct Dyn 2016;45(1):45–68.
38. **Vamvatsikos Dimitrios, Cornell C Allin**. Incremental dynamic analysis. EarthquakeEng Struct Dyn 2002;31(3):491–514
39. **Mander JB, Dhakal RP, Mashiko N, Solberg KM**. Incremental dynamic analysis applied to seismic financial risk assessment of bridges. Eng Struct2007;29(10):2662–7
40. **Chomchuen Prakit, Boonyapinyo Virote.** Incremental dynamic analysis with multimodes for seismic performance evaluation of RC bridges. Eng Struct2017;132:29–43
41. **Kazemi F, Mohebi B, Yakhchalian M.** Evaluation of the P-delta effect oncollapsecapacity of adjacent structures subjected to far-field ground motions.CivilEngJ2018;4(5):1066–73.
42. performance ofadjacent pounding structures using viscous dampers. In: The16thEuropeanConference on Earthquake Engineering; 2018. p. 18–21
43. **Kostov M.** Seismic fragility analyses. In "Regional Workshop On ExternalEventsPSA 6-10 November 2000, Sofia," 2000
44. **Duan X, Pappin JW.** "A procedure for establishing fragility functions for seismicloss estimate of existing buildings based on nonlinear pushover analysis,"in14thWorld Conference on Earthquake Engineering. Beijing: China; 2008. p. 12–7
45. **Kumitani S, Takada T.** Probabilistic assessment of buildings damage consideringaftershocks of earthquakes. 14th World Conference on EarthquakeEngineering.2008.
46. **Haran Pragalath DC, Davis R, Sarkar P.** Reliability evaluation of RC framebytwomajor fragility analysis methods. Asian J. Civil Eng. (BuildingAndHousing)2015;16:47–66.
47. Ioannou Ioanna, Douglas John, Rossetto Tiziana. Assessing the impact of groundmotion variability and uncertainty on empirical fragility curves.SoilDynEarthquake Eng 2015;69:83–92.
48. **Kappos Andreas J, Panagopoulos Georgios, Panagiotopoulos Christos,**

Penelis Gregorios. A hybrid method for the vulnerability assessment of R/CandURM buildings. Bull Earthq Eng 2006;4(4):391–413.

49. **Muntasir Billah AHM, Shahria Alam M.** Seismic fragility assessment of highway bridges: a state-of-the-art review. Struct Infrastruct Eng 2015;11(6):804–32.
50. **Ibrahim Yasser E, El-Shami Mostafa M.** Seismic fragility curves for mid-risereinforced concrete frames in Kingdom of Saudi Arabia. IES J PartA:CivilStructEng 2011;4(4):213–23.
51. **Shinozuka M, Feng MQ, Kim H-K, Kim S-H.** Nonlinear static procedurefor + fragilitycurve development. JEngMech 2000; 126 (12):1287–95.
52. **Shinozuka M, Feng M, Kim H, Uzawa T, Ueda T.** "Statistical analysis offragilitycurves. Technical Report." Multidisciplinary Center for Earthquake Engineering Research, MCEER-032003.
53. **Xue Q, Wu C-W, Chen C-C, Chen K-C.** The draft code for performance-based seismic design of buildings in Taiwan. Eng Struct 2008;30(6):1535–47.
54. COSMOSVirtualDataCenter.:⟨http://strong motioncenter.org/vdc/scripts/de